Subunit-dependent modulation of septin assembly: Budding yeast septin Shs1 promotes ring and gauze formation

Galo Garcia III,[1] Aurelie Bertin,[1] Zhu Li,[1] Yi Song,[1] Michael A. McMurray,[1] Jeremy Thorner,[1] and Eva Nogales[1,2,3]

[1]Division of Biochemistry and Molecular Biology, Department of Molecular and Cell Biology, University of California, Berkeley, Berkeley, CA 94720
[2]Life Science Division, Lawrence Berkeley National Laboratory, Berkeley, CA 94720
[3]Howard Hughes Medical Institute, Chevy Chase, MD 20815

Septins are conserved guanosine triphosphate–binding cytoskeletal proteins involved in membrane remodeling. In budding yeast, five mitotic septins (Cdc3, Cdc10, Cdc11, Cdc12, and Shs1), which are essential for cytokinesis, transition during bud growth from a patch to a collar, which splits into two rings in cytokinesis and is disassembled before the next cell cycle. Cdc3, Cdc10, Cdc11, and Cdc12 form an apolar octameric rod with Cdc11 at each tip, which polymerizes into straight paired filaments. We show that Shs1 substitutes for Cdc11, resulting in octameric rods that do not polymerize into filaments but associate laterally, forming curved bundles that close into rings. In vivo, half of *shs1Δ* mutant cells exhibit incomplete collars and disrupted neck filaments. Importantly, different phosphomimetic mutations in Shs1 can either prevent ring formation or promote formation of a gauzelike meshwork. These results show that a single alternative terminal subunit is sufficient to confer a distinctive higher-order septin ultrastructure that can be further regulated by phosphorylation.

Introduction

Septins are GTP-binding proteins conserved in all eukaryotes, except plants (Barral and Kinoshita, 2008; McMurray and Thorner, 2008; Nishihama et al., 2011). Septins participate in a wide variety of cellular processes that require membrane remodeling, ranging from bud emergence and cytokinesis in yeast (Hartwell, 1971; Slater et al., 1985) to dendritic spine formation (Xie et al., 2007) and ciliogenesis (Hu et al., 2010; Kim et al., 2010) in animal cells. Septins appear to have three primary functions. One is to erect a cortical diffusion barrier, like the septin collar at the bud neck of *Saccharomyces cerevisiae*, which prevents proteins associated with the mother cell cortex from diffusing into the bud and vice versa (Barral et al., 2000; Takizawa et al., 2000; Dobbelaere and Barral, 2004). A second is to serve as a scaffold to recruit proteins required for the execution of critical cellular processes to particular subcellular locations (Longtine et al., 1996; Shulewitz et al., 1999; Gladfelter et al., 2001; Osman et al., 2002; Nagata and

Inagaki, 2005; McMurray and Thorner, 2009). A third role for septins is to alter membrane curvature, either directly by deforming membranes or indirectly by recruiting proteins that carry out this function (Warenda and Konopka, 2002; Tanaka-Takiguchi et al., 2009).

Although not always considered part of the cytoskeleton, septins polymerize into higher-order assemblies and, in so doing, provide organization and structure to the cell. As first visualized by negative staining of serial thin sections in the electron microscope, filament-like striations are present at the neck of budding yeast cells (Byers and Goetsch, 1976). These presumptive filaments were 10 nm wide and spaced ∼28 nm apart. The *Saccharomyces cerevisiae* genome encodes seven septin genes, five of which are expressed during mitosis—Cdc3, Cdc10, Cdc11, Cdc12, and Shs1 (Haarer and Pringle, 1987; Mino et al., 1998). In cells with a temperature-sensitive mutation in *CDC3*, *CDC10*, *CDC11*, or *CDC12*, chains of multiple elongated buds are formed at the restrictive

The Rockefeller University Press $30.00
J. Cell Biol. Vol. 195 No. 6   993–1004
www.jcb.org/cgi/doi/10.1083/jcb.201107123

JCB   **993**

temperature, which do not separate from the parental cell or each other because of a failure of cytokinesis (Hartwell, 1971; Hartwell et al., 1974). The 10-nm filaments at the bud neck disappear when temperature-sensitive *cdc3*, *cdc10*, *cdc11*, or *cdc12* mutants are shifted to the restrictive temperature (Byers and Goetsch, 1976), indicating that these gene products are required for neck filament formation. Subsequent visualization of Cdc3, Cdc10, Cdc11, and Cdc12 by immunolocalization and fusion to fluorescent marker proteins demonstrated that these proteins are integral components of the neck filaments (Pringle, 2008). Furthermore, native septin complexes purified from yeast (Sanders and Field, 1994; Frazier et al., 1998) and recombinant complexes containing Cdc3, Cdc10, Cdc11, and Cdc12 expressed in and purified from bacteria (Versele et al., 2004; Farkasovsky et al., 2005) are able to self-assemble in vitro into filaments that closely resemble those observed in vivo (Bertin et al., 2008).

In contrast, the septin encoded by the *SHS1* gene has been considered nonessential because an *shs1Δ* mutant is viable and displays only a mild phenotype under normal culture conditions (30°C; Carroll et al., 1998; Mino et al., 1998). Yet, several observations suggest that Shs1 may have regulatory functions. In certain strain backgrounds, lack of Shs1 causes cold-sensitive growth (Iwase et al., 2007), and cells lacking both Shs1 and Cdc10 are inviable (Iwase et al., 2007; McMurray et al., 2011). Shs1 reportedly associates with several other nonessential factors implicated in cell polarity determination, cytokinesis, and mitotic regulation, such as Spa2 (Mino et al., 1998), Myo1 (Iwase et al., 2007), and Nis1 (Iwase and Toh-e, 2001), respectively. Moreover, Shs1 undergoes more marked phosphorylation during the cell cycle than any other septin (Egelhofer et al., 2008). The latter point is particularly relevant because mutation of protein kinases that phosphorylate septins results in aberrant septin organization at the bud neck (Barral et al., 1999; Mortensen et al., 2002; Dobbelaere et al., 2003; Versele et al., 2004).

The septin family is defined by a globular GTP-binding domain that includes structural elements unique to this class of GTP-binding protein (Sirajuddin et al., 2007, 2009) and other characteristic sequence features (Versele and Thorner, 2005; Pan et al., 2007). Septins have an N-terminal extension of variable length, and all the septins except Cdc10 possess a flexible C-terminal extension (CTE) that contains a predicted coiled coil (Versele et al., 2004; Barth et al., 2008). Regardless of species, septin subunits interact with each other to form ordered rods; the resulting rods are apolar (have a twofold rotational symmetry about a central axis orthogonal to the rod). The number of protomers per rod is different for different organisms. For example, the *Caenorhabditis elegans* genome encodes only two septins that form a linear UNC59–UNC61–UNC61–UNC59 heterotetramer (John et al., 2007), whereas the four essential *S. cerevisiae* septins form a linear Cdc11–Cdc12–Cdc3–Cdc10–Cdc10–Cdc3–Cdc12–Cdc11 heterooctamer. In vitro, three human septins form a linear SEPT7–SEPT6–SEPT2–SEPT2–SEPT6–SEPT7 heterohexamer (Sirajuddin et al., 2007); however, the human genome encodes 14 septin genes, and the combinatorial possibilities for additional arrangements are quite large (Kinoshita, 2006; Estey et al., 2011; Sellin et al., 2011).

Along the long axis of the rod, the subunit–subunit contacts alternate between a G interface (in which two guanine nucleotides are docked between each monomer) and an NC interface (in which interaction is mediated by intertwining of the N and C termini of two globular domains; Sirajuddin et al., 2007, 2009). In the yeast rod, the Cdc11–Cdc12 contact is a G interface, the Cdc12–Cdc3 contact is an NC interface, and so forth, to the other end of the rod (Bertin et al., 2008). At low salt concentration, the rods polymerize end to end via Cdc11–Cdc11 contact (an NC interface) and "zipper up" in a highly cooperative fashion to form very long paired filaments (in which the side by side pairing is mediated by cross-filament coiled coils formed by the CTEs of Cdc3 and Cdc12; Bertin et al., 2008). To date, no biochemical studies have addressed how Shs1 may influence the assembly and filament-forming capacity of septin complexes.

From several lines of evidence, we envisioned that Shs1 could interact with the other four mitotic septins by simply replacing Cdc11, forming Shs1–Cdc12–Cdc3–Cdc10–Cdc10–Cdc3–Cdc12–Shs1 heterooctamers. First, at the primary sequence level, Shs1 is most similar to Cdc11 and more divergent from the other budding yeast septins (Pan et al., 2007; McMurray and Thorner, 2008). Second, as judged by the yeast two-hybrid method (Fields, 2009; Golemis et al., 2011), Shs1 interacts most strongly with Cdc12 and only weakly with Cdc3, Cdc10, and Cdc11 (Iwase et al., 2007). Finally, in pull-down experiments from cell extracts, the amount of Shs1 present in the complexes recovered is anticorrelated with the amount of Cdc11 present—when Shs1 is pulled down, Cdc11 is substoichiometric compared with the other septins present, and conversely, when Cdc11 is pulled down, Shs1 is substoichiometric (Mortensen et al., 2002; Sung et al., 2005). These findings indicated that Shs1 and Cdc11 may compete for the same site.

Here, we use a reconstituted system to investigate how Shs1 interacts with the other mitotic septins, what properties the resulting complexes exhibit, and how Shs1 influences the higher-order organization of septin assemblies. We demonstrate that Shs1 can only occupy the terminal position in the heterooctamer, i.e., it substitutes for and competes with Cdc11 for binding to Cdc12. Compared with Cdc11-containing complexes, the resulting Shs1-containing complexes exhibit markedly different properties with regard to higher-order assembly. We used mutagenesis to delineate what elements in Shs1 are necessary to confer these unique properties. Furthermore, as a surrogate for preparing Shs1 fully phosphorylated at various positions, we examined the effect of phosphomimetic mutations to explore the potential of phosphorylation for regulating how Shs1 affects the supramolecular organization of septins. Finally, we find by both fluorescence microscopy and EM that the septin collars are clearly abnormal in a substantial fraction of the cells in a culture of an *shs1Δ* mutant. These findings have important implications for understanding the physiological roles of alternative septin subunits and their posttranslational modification.

Results

Shs1 substitutes for Cdc11 at the terminal position in septin heterooctamers

As our first approach to investigate the role of Shs1 in the organization and function of septin complexes, Shs1 was coexpressed with different combinations of the other mitotic septins in bacterial cells, as described in detail in Materials and methods, and the nature and arrangement of the resulting complexes were analyzed. We found that only when Shs1 was coexpressed with Cdc3, Cdc10, and His$_6$-Cdc12 (as the limiting subunit) was a stable complex containing Shs1, Cdc3, Cdc10, and His$_6$-Cdc12 in stoichiometric amounts recovered after our standard three-step chromatographic purification (nickel affinity, size exclusion, and ion exchange) as judged by SDS-PAGE and Coomassie staining (Fig. S1 A, left). When visualized by negative-stain EM in a high-salt (300 mM NaCl) buffer, the Shs1-containing complex possessed a rod shape (Fig. S1 B) with dimensions very similar to those of Cdc11-containing heterooctamers prepared in the same manner (Fig. S1 C).

Individual particles in such fields were examined by EM, computationally aligned, and classified into groups (classes) with distinct features. The particles in each of these classes were averaged to produce an image (class average) representative of the particles in that group and having increased signal to noise ratio. All of the class averages for the Shs1-containing complex exhibited a rod shape with no evidence of any additional density on its periphery (Fig. 1, A [right] and B). When compared with the hexameric complex composed of Cdc3, Cdc10, and Cdc12 (Fig. 1, A [middle] and C), most of the Shs1-containing complexes were two subunits longer, just like Cdc11-containing heterooctamers (Fig. 1 A, left). In addition, different class averages showed a variety of curvatures (Fig. 1 B), indicating a certain degree of flexibility along the axis of the rod, just as we observed for Cdc11-containing rods (Bertin et al., 2008). However, we observed that unlike Cdc11-containing complexes, which are almost exclusively heterooctamers, the preparation of Shs1-containing complexes also exhibited a significant proportion of heptamers and hexamers (Fig. 1 C), suggesting that Shs1 may have a lower affinity for Cdc12 than does Cdc11 and that there is an equilibrium between free Shs1, hexamers lacking Shs1, heptamers containing Shs1 at one end, and full-length heterooctamers capped with Shs1 at both ends. Similarly, it has been found recently that human septin complexes in vivo are a mixture of Sept7–Sept6–Sept2–Sept2–Sept6–Sept7 heterohexamers and Sept9–Sept7–Sept6–Sept2–Sept2–Sept6–Sept7–Sept9 heterooctamers (Sellin et al., 2011). In any event, the most parsimonious explanation for these results is that Shs1 occupies and thus can replace Cdc11 as the terminal subunit in septin heterooctamers. Interestingly, because Cdc3–Cdc10–Cdc12 complexes are exclusively hexamers (Fig. 1 C), the Cdc10–Cdc10, Cdc10–Cdc3, and Cdc3–Cdc12 interactions must all be stronger than either the Cdc11–Cdc12 or Shs1–Cdc12 association.

Shs1 promotes septin bundling and ring formation in vitro

When diluted into a buffer of low ionic strength (10 mM NaCl), Cdc11-containing rods polymerize end to end into long straight
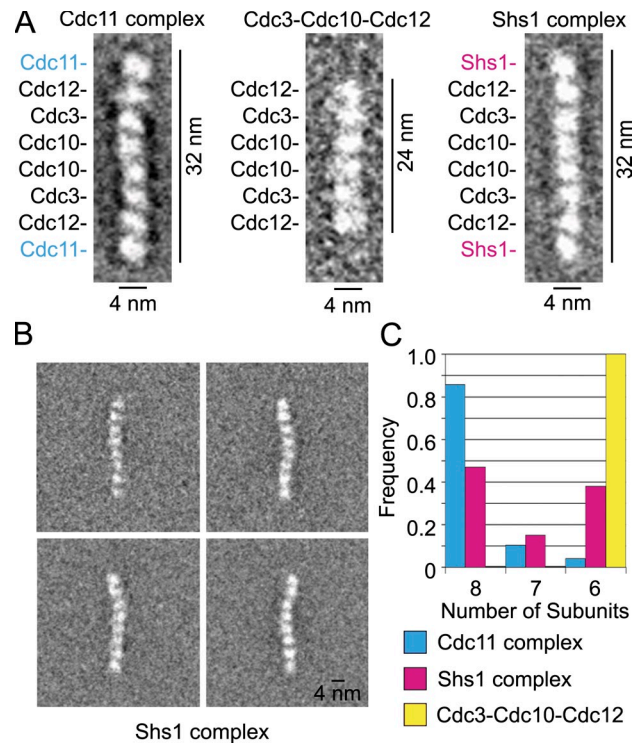

Figure 1. **Shs1 substitutes for Cdc11 at the terminal positions in septin octamers.** (A) Representative class averages of EM images of septin complexes in high salt (300 mM NaCl). (left) Cdc11-containing complex; (middle) Cdc3–Cdc10–Cdc12 hexameric complex; (right) Shs1-containing complex. Dimensions are indicated. (B) Additional class averages of Shs1-containing complexes; note the range of curvatures. (C) Histogram of the size distribution (number of subunits) for Shs1- and Cdc11-containing complexes and the Cdc3–Cdc10–Cdc12 complex. Each of the three preparations (10 µg/ml) was applied to EM grids and examined as in Fig. S1 B. Particles were assigned to classes, each with a homogeneous population of particle size, and the number of particles within each class for each preparation was counted. Cdc11-containing complex (4,211 particles total): 86% octamers, 10% heptamers, and 4% hexamers. Shs1-containing complex (9,901 particles total): 47% octamers, 15% heptamers, and 38% hexamers. Cdc3–Cdc10–Cdc12 complex (2,093 particles total): 100% hexamers.

filaments that pair (Fig. 2 A). In contrast, the hexameric Cdc3–Cdc10–Cdc12 complex does not form any higher-order structures under either of these in vitro conditions (this study; Bertin et al., 2008). To determine the self-assembly properties of Shs1-containing complexes, the purified preparation maintained in high salt buffer was diluted in low salt buffer. Strikingly, when examined by EM, we found that the Shs1-containing complexes formed no paired filaments but instead assembled into large, multilayered ringlike structures ($n = 109$) with a mean outer diameter of 410 ± 53 nm and a mean inner diameter of 267 ± 49 nm (Fig. 2 B). The ringlike ensembles must be composed of Shs1-containing heterooctamers, as judged by the fact that EM analysis of the particles (2,115 total) on the grid that were not incorporated into the rings (Fig. S2) revealed that they are mostly hexamers (78%) with a small proportion of heptamers (15%) and very few octamers (6%).

To investigate the time course of formation of these novel structures, purified Shs1-containing complexes in high salt were diluted into low salt buffer at 4°C, and samples were withdrawn at various time intervals and then fixed, stained, and viewed in the EM. Within the shortest time permitted by these manipulations
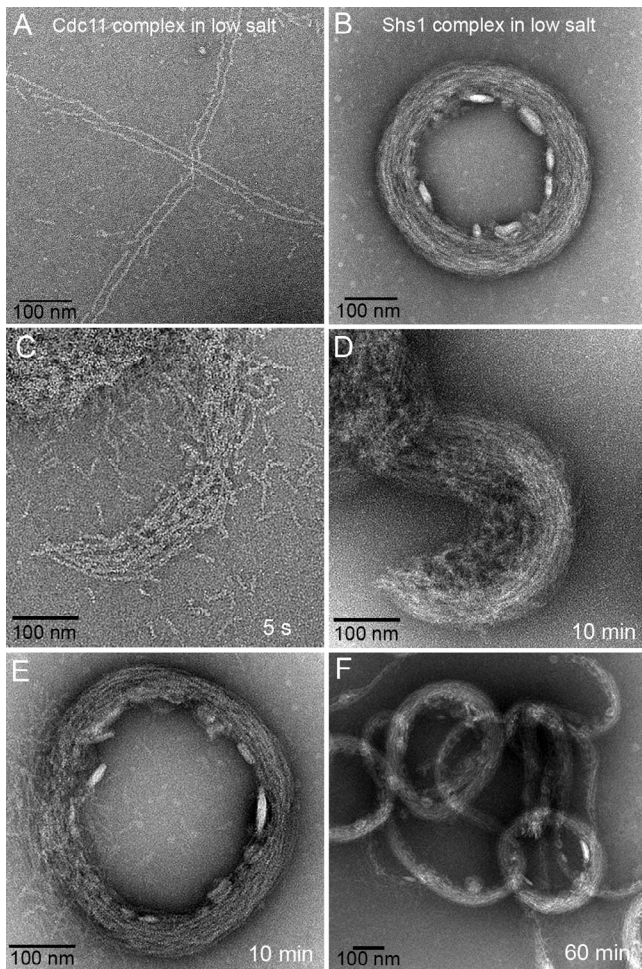
Figure 2. **Shs1 promotes formation of rings under low salt conditions.** (A) A sample of Cdc11-containing complexes was diluted from high salt conditions into low salt buffer, as described in Materials and methods, applied to EM grids, and examined as in Fig. S1 B. (B) A sample of the Shs1-containing complex was treated as in A. (C–F) Time course of ring and spiral formation by Shs1-containing complexes. A sample of a preparation of Shs1-containing complexes in a high salt complex was diluted as in B into low salt at 4°C, and samples were taken at the indicated times—5 s (C), 10 min (D and F), and 60 min (F)—and immediately applied to EM grids and examined. Note the scale bar difference in F.

(5 s), curved bundles were formed, in which it was evident that the rods interact both end on end and laterally (often in a staggered manner, allowing for further longitudinal extension; Fig. 2 C). By 10 min, the loose bundles of short staggered filaments have become more tightly packed, side to side, and have extended into prominent arcs (Fig. 2 D) and closed rings (Fig. 2 E). By 60 min, those arcs that had not closed on themselves to form rings were able to extend into luxuriant spirals (Fig. 2 F). We never observed longer than octamer-length rods or any filaments in the background of the arcs, rings, and spirals, indicating that end to end polymerization into the short curved filaments found in the bundles can only occur concomitantly with their lateral interaction.

Ring formation requires both the N terminus and the CTE of Shs1

When Cdc11-containing complexes polymerize into filaments, the Cdc11 subunit at the end of each octamer associates with

the Cdc11 at the end of the neighboring octamer via an NC interface. The α0 helix (as defined by Sirajuddin et al., 2007) at the N terminus of Cdc11 makes a major contribution to this interface, and deletion of the corresponding residues does not prevent Cdc11 folding or incorporation into complexes but does prevent polymerization of the resulting mutant octamers into filaments (Bertin et al., 2008). In contrast, deletion of the C-terminal residues of Cdc11 corresponding to nearly its entire CTE has no deleterious effect on either octamer assembly or filament formation (Bertin et al., 2008). To begin to dissect the molecular requirements by which Shs1 mediates the novel interactions that lead to ring formation, we generated both an α0 deletion mutation, Shs1(Δ2–18), and a truncation that removed its CTE, Shs1(Δ349–551), and then assessed the ability of these mutants to assemble into complexes and, if formed, the capacity of those complexes to generate the higher-order structures formed by complexes containing wild-type (WT) Shs1. Both Shs1(Δ2–18) and Shs1(Δ349–551) were expressed in stable form, indicating their proper folding, and both were incorporated into heterooctamers when coexpressed with Cdc3, Cdc10, and His$_6$-Cdc12 just as well as intact Shs1 (Fig. 3 A), as expected, because neither of these mutations should perturb the G interface by which Shs1 interacts with Cdc12. Interestingly, Shs1(ΔCTE)-containing complexes form more stable octamers (72% octameric) than WT Shs1-containing complexes (47% octameric), which suggests that the C-terminal of extension of Shs1 somewhat destabilizes the interaction between Shs1 and Cdc12 at the G-interface under the high salt conditions used in this assay. However, neither the complexes containing the α0 helix deletion mutant (Fig. 3 B) nor those containing the CTE truncation mutant (Fig. 3 C) were able to support the bundle formation or ring assembly displayed by complexes containing intact Shs1 under the same conditions (Fig. 3 D). Thus, the septin–septin interactions responsible for forming these unique structures require both the N and C termini of Shs1.

Shs1 is important for organization of the septin collar in vivo

Given our in vitro findings demonstrating that substitution of Cdc11 with Shs1 has such a dramatic effect on how the resulting heterooctamers assemble into higher-order structures, we examined the issue of whether absence of Shs1 perturbs the arrangement of the other septin subunits in situ. To visualize septin collars at the light microscope level, *SHS1+* and otherwise isogenic *shs1Δ* cells expressing Cdc11-GFP from the *CDC11* promoter on a *CEN* plasmid as the sole source of this septin were examined under the fluorescence deconvolution microscope. Because septin structures disassemble after cytokinesis, we scored only budded cells, in which the septin collar (or the rings arising from splitting of the collar before cytokinesis) is a normally prominent and readily discernible structure. Indeed, in *SHS1+* cells, Cdc11-GFP was found in collars and split rings of uniform shape and integrity (Fig. 4 A). In contrast, in *shs1Δ* cells, the distribution of Cdc11-GFP exhibited marked abnormalities, including discontinuous rings, peripheral clumps, and barlike structures oriented in apparently random directions (Fig. 4 B). In the fields examined, none of the Cdc11-GFP–expressing *SHS1+* cells
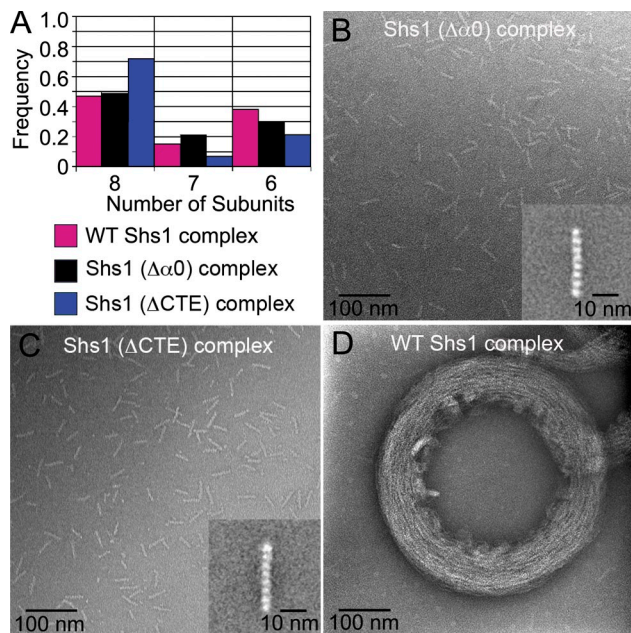
Figure 3. **Ring formation requires both the α0 helix and the CTE of Shs1.** (A) Purified complexes containing either WT Shs1, Shs1(Δα0), or Shs1(ΔCTE) in high salt were examined in the EM. The histogram shows the size distribution (number of subunits) determined as in Fig. 1 C. Shs1(Δα0)-containing complex (2,241 particles total): 49% octamers, 21% heptamers, and 30% hexamers. Shs1(ΔCTE)-containing complex (4,027 particles total): 72% octamers, 7% heptamers, and 21% hexamers. Samples of each of these three preparations were diluted into low salt conditions for 30 min and then applied to grids and examined in the EM. (B–D) Representative fields are shown for Shs1(Δα0; B), Shs1(ΔCTE; C), and WT Shs1 (D). Representative octameric class averages are shown for Shs1(Δα0; B) and Shs1(ΔCTE; C) in the insets.

Figure 4. **Lack of Shs1 disrupts septin collar organization at the light microscope level.** (A–D) Either *SHS1+* (left) or *shs1Δ* (right) cells expressing either Cdc11-GFP from the *CDC11* promoter on a *CEN* plasmid (A and C) or Cdc10-mCherry from the *CDC10* promoter at the *CDC10* locus on chromosome III (B and D) were examined by fluorescence deconvolution microscopy. Arrows point to aberrant septin collars. Dotted lines outline cells. Bars, 2 µm. (E) Fraction of *SHS1+* and *shs1Δ* cells displaying abnormal collars with either Cdc11-GFP or Cdc10-mCherry as indicated. The data shown are from a single representative experiment out of two replicates.

displayed any such defects, whereas virtually all of the Cdc11-GFP–expressing *shs1Δ* cells did (Fig. 4 E). To corroborate this finding, we also examined *SHS1+* and otherwise isogenic *shs1Δ* cells expressing Cdc10-mCherry from the *CDC10* promoter at its endogenous locus as the sole source of this septin. Again, in all of the *SHS1+* cells, Cdc10-mCherry was found in collars and split rings of uniform shape and integrity (Fig. 4 C), whereas in *shs1Δ* cells (Fig. 4 D), the distribution of Cdc10-mCherry was disrupted and clearly abnormal in nearly half of the cells (Fig. 4 E). Nonetheless, even with these apparent defects in septin organization, the cells lacking Shs1 had a doubling time equivalent to the *SHS1+* parental strain and did not produce elongated buds.

To gain further insight, we examined organization of the septin-containing 10-nm filaments at the bud neck (Byers and Goetsch, 1976) in *SHS1+* and *shs1Δ* cells at the ultrastructural level in fixed and stained thin sections using EM and electron tomography by methods that are described in detail elsewhere (Murray, 2008). Unlike *SHS1+* cells, in which highly organized striations corresponding to the 10-nm filaments orthogonal to the bud neck can be readily found in grazing thin sections (Fig. 5, A and B), no such structures could be visualized in similar sections of *shs1Δ* cells. When thicker sections were viewed by electron tomography, individual slices (Fig. 5, C and D) and the resulting model generated by tomographic reconstruction (Video 1) revealed that 10-nm filaments are still present at the
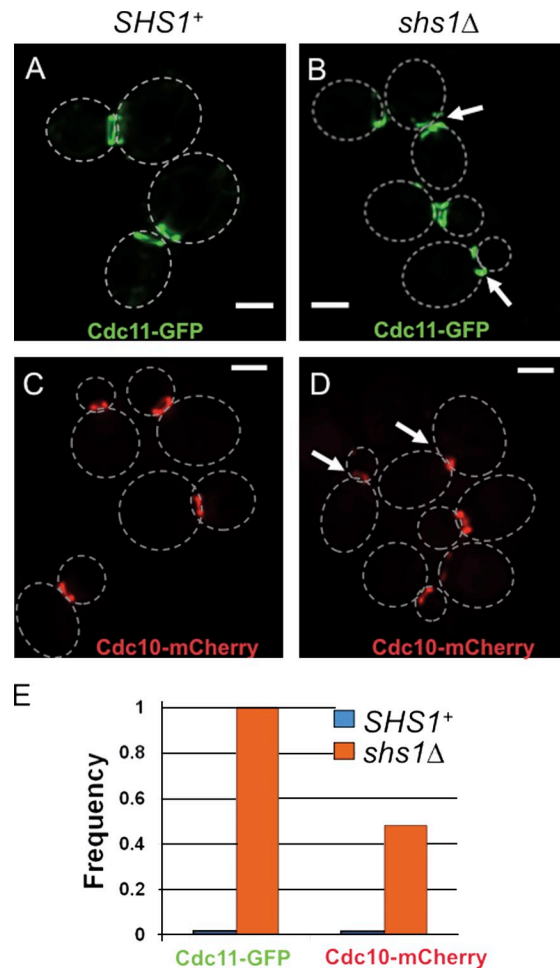
bud neck in *shs1Δ* cells, but these are much less organized compared with the well-ordered arrays found in WT cells (not depicted). In *shs1Δ* cells, continuous 10-nm filaments are no longer arranged around the circumference of the bud neck perpendicular to the mother–bud axis but rather are "broken" and mostly oriented parallel or at various angles with respect to the mother–bud axis. Thus, in agreement with our in vitro data, our observations at both the cellular and ultrastructural level indicate that Shs1 has a significant role in organizing the septin filaments into well-ordered arrays that completely encircle the cell cortex at the bud neck to form the ringlike structures that compromise the septin collar.

Relative stoichiometry of Cdc11 and Shs1 influences septin ring diameter in vitro

Based on our finding that Shs1 occupies the same terminal position in septin heterooctamers as Cdc11, it seems likely
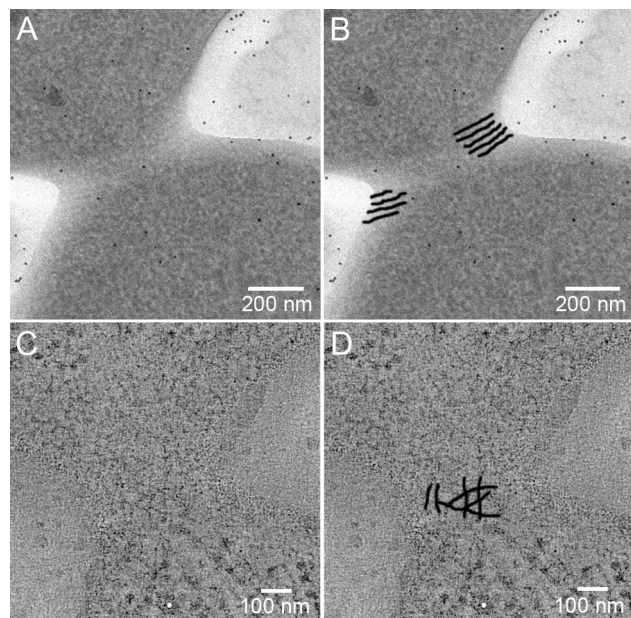
Figure 5. **Lack of Shs1 disrupts septin collar organization at the EM level.** Samples of *SHS1+* and *shs1Δ* cells were processed and examined by EM and EM tomography as described in Murray (2008) and in Materials and methods. (A) Grazing thin section of *SHS1+* cell. (B) The same image as in A with neck filaments traced in black. (C) A slice through a tomogram of an *shs1Δ* cell; note the disorganized filaments at the bud neck. (D) The same slice as in C with filaments traced in black.

Figure 6. **Relative stoichiometry of Shs1 and Cdc11 modulates septin ring diameter.** Shs1-containing complexes (S) were mixed with increasing amounts of Cdc11-containing complexes (C) in high salt in the ratios indicated. The resulting mixtures were diluted into low salt buffer and then examined in the EM. (A) Shs1-containing complex alone; mean outer ring diameter of 410 ± 53 nm (*n* = 109). (B) 9:1 ratio; mean outer ring diameter of 608 ± 86 nm (*n* = 80). (C) 5:1 ratio; mean outer ring diameter of 692 ± 92 nm (*n* = 48 nm); (D) 3:1 ratio; mean outer ring diameter of 846 ± 141 nm (*n* = 44). (E) 1:1 ratio; no rings. (F) Cdc11-containing complex alone. (G) Values obtained in A–D plotted as a histogram. Error bars are the standard deviations.

that, in mitotically growing cells (in which Cdc3, Cdc10, Cdc11, Cdc12, and Shs1 are all expressed), three types of septin octamers coexist: septin rods with Cdc11 at one end and Shs1 at the other and rods containing Cdc11 at both ends or Shs1 at both ends. To assess the effects of changing the relative stoichiometry of Shs1 and Cdc11, we investigated in vitro the effect of mixing purified Shs1-containing octamers and Cdc11-containing octamers, in varying proportions, on the assembly of higher-order structures. For this purpose, the Shs1-containing complexes were mixed with increasing amounts of Cdc11-containing complexes in high salt, and the resulting mixtures were diluted into low-salt buffer and then examined in the EM. We noted, first, that increasing the proportion of Cdc11-containing rods to Shs1-containing rods (even ≤25%) did not prevent ring formation (Fig. 6). Strikingly, however, raising the ratio of Cdc11-containing rods to Shs1-containing rods increases the diameter (and may reduce the thickness) of the resulting rings (Fig. 6, A–D and G). Thus, mixing a complex that associates into rings with one that polymerizes into long straight filaments caused radial enlargement of the rings in a dose-dependent manner. When we mix Shs1-tipped rods and Cdc11-tipped rods in a 1:1 ratio, we observe only paired straight filaments (Fig. 6 E), indicating that there is a maximum ratio of the two complexes over which rings are no longer formed. The paired filaments that form in the presence of Shs1-containing complexes show repeating densities with octamer periodicity (every 33 ± 3 nm, *n* = 132) that bridge the filaments (Fig. 6 E) and that are never seen for pure Cdc11-containing septin rods. Similar densities (with an indistinguishable repeat
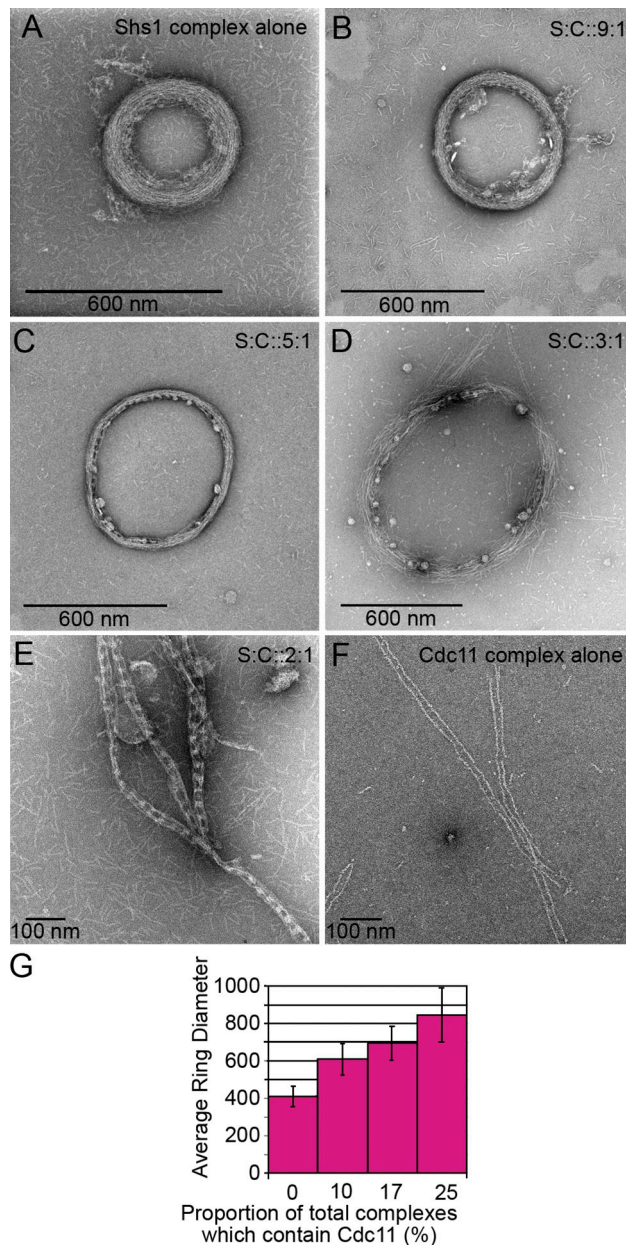
length of 33 ± 3 nm, *n* = 104) are also observed at the inner surface of septin rings made of mixed complexes (Fig. 6, B and C), which, again, are not present in rings containing Shs1 complexes alone. Thus, although we do not know for certain the precise nature of these densities, it is likely that they correspond to the Shs1 protein interacting with Cdc11, most probably via their coiled coils.

Phosphomimetic mutations suggest that modification of Shs1 could strongly influence higher-order septin architecture

There is evidence from in vitro assays, in vivo studies, and proteomic analysis that several of the mitotic septins are phosphoproteins and direct substrates of protein kinases that seem to contribute to the efficiency and/or temporal dynamics of higher-order septin assembly, including Cdk1/Cdc28 (Tang and Reed, 2002; Fiedler et al., 2009; Holt et al., 2009), Cla4 (Schmidt et al., 2003; Versele et al., 2004), and Gin4 (Mortensen et al., 2002; Asano et al., 2006). However, Shs1 appears to be the mitotic septin that undergoes the greatest degree of posttranslational modification by phosphorylation (Egelhofer et al., 2008).

For the aforementioned reasons, we generated Shs1 phosphomimetic mutants (Ser or Thr to Asp) based on in vivo phosphosites mapped by mass spectrometry (Egelhofer et al., 2008), prepared complexes containing these Shs1 mutants, diluted them into low salt buffer, and visualized the resulting structures by EM in the usual manner. The Shs1 mutants analyzed were P1, a single mutation (T6D) near the Shs1 N terminus; P2, T6D plus four sites in the CTE (T386D, S416D, S441D, and S447D; the inverse of a T6A, T386A, S416A, S441A, and S447A mutant described previously; Egelhofer et al., 2008); P3, P2 plus eight more sites in the CTE (T6D, T386D, S416D, S441D, S447D, S460D, T462D, S519D, S520D, S521D, S522D, S525D, and S545D); and, P4, a single mutation (S259D) at the Shs1 NC interface. All of these Shs1 variants were incorporated into octamers with an efficiency in the same range as WT Shs1. The P1-containing complex formed rings indistinguishable from those formed by WT Shs1-containing complexes (Fig. 7 A), whereas the P2 mutant complex formed only poorly ordered rings (Fig. 7 B), and the P3 mutant complex formed no rings at all (Fig. 7 C). This inhibition of ring formation was not caused by dissociation of Shs1 from the complex; for example, in the preparation of P2 and P3 complexes, most were clearly still octameric (61% of P2 complexes, 1,693 of 2,755 particles examined; 50% of P3 complexes, 4,987 of 9,956 particles examined). Because we also demonstrated here that the CTE of Shs1 is required for ring formation, the properties of the P2 and P3 complexes suggest that CTE phosphorylation might negatively regulate the capacity of Shs1-containing octamers to form rings.

Strikingly, the P4 mutant complex formed both rings and a gauzelike structure with a regular repeating pattern (Fig. 7 D and Fig. S3). In these meshworks, the center to center distance between the junctions of the stacked orthogonal filaments is 28 ± 1 nm ($n = 263$ total segments measured; Fig. S3). Of all of the gauzes examined ($n = 68$), the largest we observed was six segments long, and the mean gauze size was 4 ± 1 segments long. The potential physiological relevance of this in vitro finding is that a gauzelike arrangement of filaments (attributed to septins by antibody decoration) was found at the bud neck when replicas of fixed yeast spheroplasts were examined after "unroofing" by freeze fraction and deep etching (Rodal et al., 2005). Because the P4 complex was also able to form rings (Fig. S3), there is presumably an equilibrium between rings and gauzes. Thus, the properties of the P4 complex
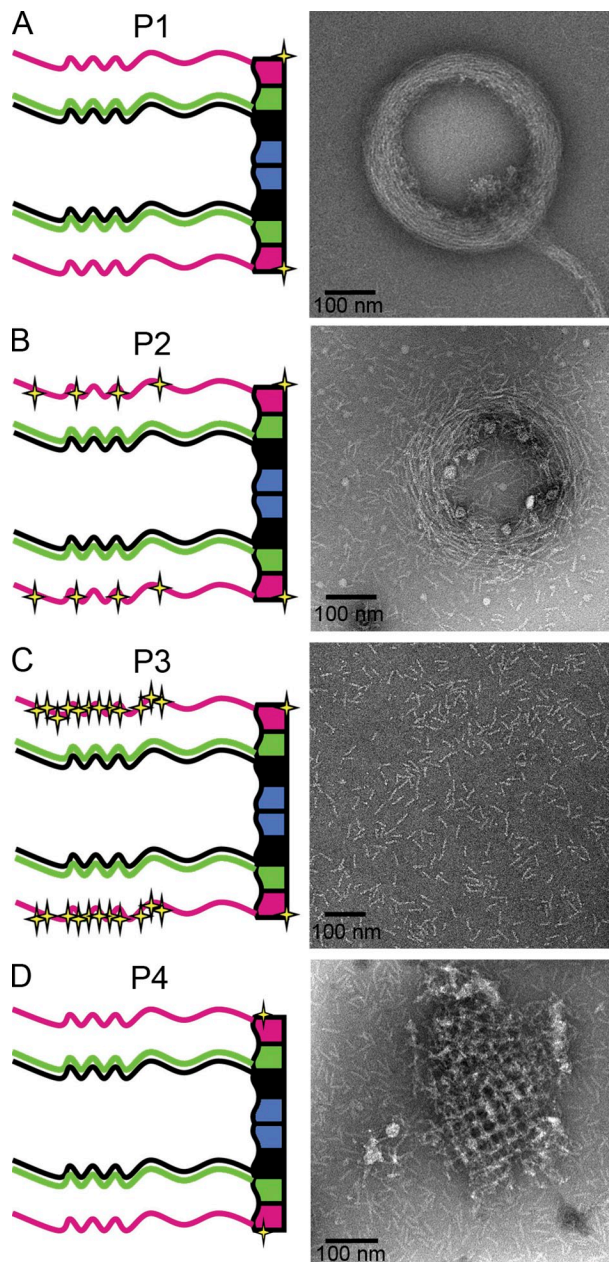

Figure 7. **Effect of phosphomimetic mutations on assembly properties of Shs1-containing complexes.** Purified septin complexes containing four different Shs1 mutants were diluted into low salt and examined in the EM. (A–D) Mutant P1, Shs1(T6D; A); mutant P2, Shs1(T6D, T386D, S416D, S441D, and S447D; B); mutant P3, Shs1(T6D, T386D, S416D, S441D, S447D, S460D, T462D, S519D, S520D, S521D, S522D, S525D, and S545D; C); and mutant P4, Shs1(S259D; D). Micrographs depict representative images. Schematic diagrams on the left indicate the order of septin subunits (Shs1, magenta; Cdc12, green; Cdc3, black; Cdc10, blue), and the positions of each phosphomimetic mutation are shown as yellow stars.

suggest that phosphorylation of Shs1 on Ser259 might act as a molecular switch to shift septin ensembles between different states of organization.

Discussion

We have shown here that Shs1 substitutes for Cdc11 at the terminal position in yeast septin heterooctamers and is solely

responsible for promoting a novel form of self-assembly, namely the formation of rings. A mammalian hexameric septin complex composed of Sept2, Sept6, and Sept7 was also reported to form rings in vitro (Kinoshita et al., 2002). Like deletion of its CTE, increased negative charge in this region of Shs1, as might arise from the known phosphorylation in this segment (Egelhofer et al., 2008), blocks ring assembly. Conversely, a single new negative charge at the NC interface of Shs1 dramatically alters the assembly properties of Shs1-containing complexes, promoting formation of a cross-braced gauzelike arrangement. Finally, we found that absence of Shs1 clearly perturbs septin collar organization at the bud neck caused by disruption of the normal organization of the cortical septin-containing 10-nm filaments.

Alternate subunits confer functional specificity

The fact that substitution with just one new subunit and its state of modification can so dramatically affect the supramolecular arrangement of yeast septin-based structures suggests that, in other organisms (such as humans) with an even greater repertoire of septin genes, replacement of specific subunits with alternative ones will be one means for producing septin complexes with different structural properties and, hence, different functional specificity. Thus, in such cases, the presence of multiple related subunit genes is to provide for physiological plasticity rather than mere redundancy. Moreover, in mammals, septins are expressed in a developmentally regulated and cell type–specific manner (Peterson and Petty, 2010; Estey et al., 2011). For example, some septin homologues are found exclusively in the brain, whereas others are found exclusively in the testes. Thus, certain septin subunits may confer particular tissue-specific structure and function. Such substitutions could also change the scaffolding properties of septin complexes for recruitment of proteins involved in different biological processes. Indeed, in budding yeast, two septins, Spr3 (Ozsarac et al., 1995) and Spr28 (De Virgilio et al., 1996), are expressed exclusively during meiosis and sporulation. At the primary sequence level, Spr28 is most similar to Cdc11 and Shs1, whereas Spr3 is most similar to Cdc12 (Pan et al., 2007; Bertin et al., 2008). Thus, it is possible that substitution of Cdc12 by Spr3 and of Cdc11 and/or Shs1 by Spr28 might confer on septin complexes the properties necessary to form the novel septin-containing structures that encase developing ascospores (Bertin et al., 2008). Structure function studies on Spr3- and Spr28-containing septin complexes may shed further light on this hypothesis.

Insights about the properties and roles of Shs1

Because of their shared GTP-binding (G) domain, septin family members are presumed to have a very similar tertiary fold (Weirich et al., 2008). However, some septins clearly have additional structural features that distinguish them from their closest relatives. Indeed, Shs1 possesses two elements—a 31-residue insert (66–97) in its G domain and a 45-residue insert (401–446) in its CTE—that Cdc3, Cdc10, Cdc11, and Cdc12 all lack. Clearly, these structural elements may contribute to conferring

the unique properties that we have described here for Shs1-containing complexes. Thus, in the case of the septin gene family, duplication and sequence drift provided a means to maintain the overall arrangement of septin complexes yet generate differences that can be exploited to alter their higher-order organization. Incorporation of such alternative subunits provides a mechanism to achieve ultrastructural diversity because changing the composition of the complex contributes new surfaces for novel intersubunit interactions (and, potentially, for unique interactions with different sets of septin-associated proteins). In this regard, Shs1 is a close relative of Cdc11 at the primary sequence level, which presumably explains how it shares with Cdc11 the capacity to interact with Cdc12 via a G interface. Yet, Shs1 is divergent enough, perhaps because of the aforementioned inserts, that it mediates formation of distinct ultrastructures. Unlike the NC interface–mediated end to end interactions between Cdc11-containing complexes that form straight filaments, Shs1-containing complexes engage in staggered side to side interactions that provide the curvature necessary for formation of spirals and rings.

The fact that both the α0 helix in its G domain and its CTE are required for Shs1-containing complexes to form rings is also significant. Septins contain a nucleotide-binding domain, like tubulin, with which they share the property of self-assembly into linear filaments (Nogales, 2000). However, septins also contain a predicted coiled coil–forming segment in their CTE, a structural motif present in intermediate filaments, with which septin filaments share their lack of polarity and the capacity to form meshes and ropelike fibers (Goldman et al., 2008). Thus, septins may achieve their capacity for ultrastructural diversity because they possess aspects of both of these dissimilar cytoskeletal protein families, allowing higher-order, septin-based structures to achieve a unique degree of supramolecular complexity.

Aside from causing formation of a different ultrastructure, alternative subunits in septin complexes may modulate the dimensions of an existing ensemble. In vitro, the Shs1-containing complex alone forms rings having a mean diameter of 410 nm, but increasing the ratio of Cdc11-containing complexes to Shs1-containing complexes more than doubled the diameter of the rings. It is tempting to speculate that regulation of their relative stoichiometry in vivo may contribute to the size increase that the septin collar undergoes at the bud neck as the cell cycle proceeds. The diameter of the septin collar in fixed yeast is, depending on the conditions used, between 540 nm (Byers and Goetsch, 1976) and 970 nm (unpublished data), clearly in the same size range as the Shs1-containing rings we were able to achieve in vitro by increasing the content of Cdc11-containing complexes. Furthermore, during the process of membrane remodeling and surface expansion at the bud neck during cell growth and division, the arrangement of the membrane-bound septins must be sufficiently dynamic and flexible to accommodate these changes and maintain its functions. In this regard, relative Shs1 and Cdc11 stoichiometry seems to be important for establishing the hourglass shape of the septin collar at the bud neck, given that this structure was clearly disrupted in the majority of cells when Shs1 was

absent. If the hourglass is formed by stacking hoops of 10-nm filaments, the hoops at the constriction of the hourglass must have the greatest curvature and hence may have the highest content of Shs1, given its ring-promoting property. We are attempting to devise physical markers for EM and/or cryo-EM imaging to confirm this prediction in situ.

Given its conservation across fungi and the properties of Shs1 we have discovered, it was surprising that previous studies reported no dramatic phenotype of *shs1Δ* mutants (Carroll et al., 1998; Mino et al., 1998). As we have documented here, the lack of Shs1 clearly compromises the organization of the septin collar. In addition, WT *SHS1*+ and *shs1Δ* cells expressing both Sec3-GFP and Cdc10-mCherry show accumulation of Sec3-GFP between the split septin rings in WT cells but not in the *shs1Δ* cells (Fig. S4). This suggests that Shs1 is necessary to maintain Sec3 between split septin rings, a point which illustrates the association between the disorganization of the septin collar and a compromised diffusion barrier formed by split septin rings when Shs1 is absent. Nonetheless, these defects result in an unexpectedly mild phenotype, at least under laboratory conditions.

However, several observations suggest that Shs1 and its function are not truly dispensable. In particular, although otherwise WT cells can tolerate the absence of either Shs1 or Cdc10 (Frazier et al., 1998; McMurray et al., 2011) at 30°C and below, an *shs1Δ cdc10Δ* double mutant is inviable (Iwase et al., 2007; McMurray et al., 2011) under all conditions. Thus, when the stability and arrangement of the 10-nm filaments are compromised by the absence of Cdc10, the support function provided by Shs1 becomes indispensible, suggesting that Shs1 does indeed provide additional structural and organizational information required for optimal septin collar assembly and/or function.

Phosphorylation may regulate septin function by inhibiting or altering self-assembly

Our observations with phosphomimetic mutations in Shs1 suggest that phosphorylation could serve as an on/off switch for regulating the assembly state and thus the specific function of septin-based structures. Theoretically, there are at least three levels at which phosphorylation could regulate septin assembly state. First, as suggested by the Shs1 variants with phosphomimetic mutations in the CTE that assembled into complexes but no longer formed rings, phosphorylation could prevent cross-complex association and block self-assembly. Second, phosphorylation at a specific septin–septin interface could weaken the subunit–subunit interaction and thereby potentiate either complex disassembly and/or dissociation of an individual subunit and its replacement by an alternative subunit, a possibility that we did not observe in our experiments. Third, as suggested by the unique behavior of Shs1(S259D) in promoting gauze formation, phosphorylation could induce structural changes that drive novel cross-complex interactions and thereby the acquisition of a markedly different ultrastructure. The remarkable feature of the gauzelike arrangement is the regular spacing between orthogonal filament arrays. Thus, in vivo, site-specific phosphorylation of Shs1 could be responsible for maintaining a

constant distance between the circumferential septin filaments by organizing cross-braces of perpendicular septin filaments at regular intervals. Indeed, such a meshlike arrangement of septin filaments at the bud neck is a pattern we have observed by EM tomography (unpublished data). At the resolution of the septin collar visualized by fluorescence microscopy, it was not possible previously to discriminate this latticelike arrangement. However, dynamic changes in the organization of this gauzelike structure can readily explain the results of biophysical experiments that proposed that two distinct types of septin filament arrangements alternate as the cell division cycle progresses (Vrabioiu and Mitchison, 2006, 2007). Indeed, several protein kinases reportedly affect, directly or indirectly, the ability of septins to assemble (or disassemble) during the cell cycle. For example, when cells lack the protein kinase Gin4, assembly of the septin collar is significantly delayed or abortive in a significant fraction of the cells (Longtine et al., 1998; Mortensen et al., 2002; McMurray and Thorner, 2009). The attendant disruption in septin organization is manifest as barlike aggregates that run parallel to the mother–bud axis. Shs1 is known to be one of the primary cellular targets of Gin4 (Egelhofer et al., 2008). Thus, in the absence of Gin4-dependent phosphorylation, the gauzelike arrangement may collapse, perhaps because of conditions that favor bundling of the Shs1-containing filaments. Further analysis of the effects of authentic phosphorylation of Shs1 on the assembly properties of septin complexes in vitro will provide further insight about the control of septin assembly in vivo.

Materials and methods

Septin complex expression and purification

His$_6$-Cdc12 and untagged septin subunits were coexpressed in *Escherichia coli* BL21(DE3) cultures from Duet vectors (EMD). DNA encoding SHS1 was provided by E. Bi (University of Pennsylvania, Philadelphia, PA). The cultures were grown to an A_{600nm} = 0.7, induced with isopropyl-β-D-thiogalactoside (1 mM final) for 16 h at 16°C, collected by centrifugation, resuspended in lysis buffer (300 mM NaCl, 2 mM MgCl$_2$, 40 µM GDP, 0.1% monothioglycerol [MTG], 0.5% Tween 20, 12% glycerol, and 50 mM Tris-HCl, pH 8.0), and flash frozen. After thawing, the cells were added protease inhibitor mix (Complete EDTA-free; Roche) and 0.2 mg/ml lysozyme, incubated on ice for 30 min, and then sonicated with two 30-s pulses (Sonicator 3000; Misonix). Lysates were clarified at 4°C by centrifugation at 12,000 g. The resulting supernatant fraction was subjected to Ni^{2+}-affinity chromatography (HisTrap HP; GE Healthcare) in high salt buffers to prevent septin self-assembly (wash buffer: 300 mM NaCl, 20 mM imidazole, 50 mM Tris-HCl, pH 8.0, and 0.01% MTG; elution buffer: 300 mM NaCl, 300 mM imidazole, 50 mM Tris-HCl, pH 8.0, and 0.01% MTG). Size-exclusion chromatography (HiLoad 16/60 Superdex 200; GE Healthcare) was performed on the peak eluate fractions in septin buffer (300 mM NaCl, 50 mM Tris-HCl, pH 8.0, and 0.01% MTG). The peak size-exclusion eluate fractions were pooled and further purified by ion-exchange chromatography with a salt gradient ranging from 0 to 500 mM NaCl in buffers that also contained 50 mM Tris-HCl, pH 8.0, and 0.01% MTG.

EM and image processing

After purification, septin complexes were diluted to a concentration of 0.01 mg/ml in either high salt buffer (300 mM NaCl, 2 mM MgCl$_2$, and 50 mM Tris, pH 8.0) or low salt buffer (10 mM NaCl and 2 mM MgCl$_2$ or 50 mM Tris, pH 8.0). The diluted samples were absorbed onto a carbon-coated copper grid after glow discharging the grids on a thermal evaporator (Auto 306; Edwards). The grids were then washed with water and stained with 2% uranyl formate.

Electron micrographs of the sample were taken using an electron microscope (Tecnai T12; FEI) operated at 120 kV and using a 70-µm objective aperture. Unless otherwise indicated, micrographs were taken at

Table 1. Yeast strains used in this study

Strain	Genotype	Source of reference
BY4741	MATa his3Δ1 leu2Δ0 met15Δ0 ura3Δ0	Research Genetics, Inc.
JTY3498	BY4741 cdc11Δ::HIS3 pRS316-Cdc11-GFP	This laboratory
JTY4944	BY4741 cdc11Δ::HIS3 shs1Δ::KanMX pRS316-Cdc11-GFP	This laboratory
JTY5397	BY4741 Cdc10-mCherry::KanMX Shs1-GFP::His3MX6	This laboratory
JTY5207	BY4741 Cdc10-mCherry::KanMX shs1Δ::HphMX	This laboratory

30,000× magnification, with a defocus of about −1 µm. The micrographs were converted to a digital format using a scanner (Coolscan 8000; Nikon). Length measurements of rings and other features were performed using ImageJ (National Institutes of Health; Abramoff et al., 2004). Images of individual complexes were windowed out of the images with a box size of 135 × 135 pixels using the Boxer program within the EMAN (electron microscopy analysis) software package (Ludtke et al., 1999). The particles were then aligned and classified using SPIDER (Frank et al., 1996). The first round of alignment and classification was reference free, and class averages were selected to ensure full representation of the diversity in length and curvature of complexes in the sample. These class averages were used as references in subsequent iterations of alignment and classification. After each round of alignment and classification, new references were chosen from the class averages produced. Iterations of alignment and classification were continued until there were no changes in the class averages from one round to the next. To determine the distribution of particles sizes within the sample, the classes were manually assigned to groups according to the particle size, and the number of particles in each group was counted.

Electron tomography
Yeast cells that would be subsequently freeze substituted were grown in YPD (yeast, peptone, dextrose) media at 30°C until they reached exponential growth (OD of 0.4–0.6). To avoid any cell damage by centrifugation, the grown cells were concentrated to a yeast paste by vacuum filtration. After being inserted in 100-µm deep membrane carriers (Leica), the yeast paste was high pressure frozen using a high pressure freezer device (Model EM PACT2-RTS; Leica). Before use, the membrane carriers were coated with 1-hexadecene (Fluka).

Freeze substitution was performed in a device (AFS2; Leica) by raising the temperature from −90°C in increments of 2°C per hour up to −25°C and then in increments of 5°C per hour up to 0°C. 1% osmium tetroxide, 0.1% uranyl acetate, and 5% water in acetone was used as the substitution media. The samples were embedded into Epon resin. Sections of 150 and 200 nm were obtained from the Epon blocks using a microtome (Ultracut E; Reichert) equipped with a 4.5-mm diamond knife (Diatome). The sections were deposited on hexagonal copper grids with a mesh size of 100, which had been covered with Formvar. The samples were poststained using uranyl acetate 2% in methanol and lead citrate. 10-nm gold beads were deposited on both sides of the sections before a thin film of carbon was evaporated. The dual-axis tilted series were collected using a microscope (CM200 FEG; Philips) operated at 200 kV and the DigitalMicrograph software suite (Gatan, Inc.) at a magnification of 20,289×. A dual-axis tomography holder was used (model 2040; Fischione). If possible, the tilted series were collected from −70 to 70°. The resin-embedded samples were preexposed for ∼30 min before data collection to avoid any shrinkage or deformation of the plastic resin during the process. The data were processed using IMOD (Kremer et al., 1996; Mastronarde, 2008). Gold beads were used as fiducials for aligning the tilted series. The reconstructed volumes were obtained by weighted back projection before the two axes were recombined, with a voxel size of 6.9 Å. The segmentation was obtained using IMOD.

Fluorescence microscopy
The yeast strains used in this study are listed in Table 1. All strain constructions were performed with standard genetic and molecular biology methods. The strain to be examined was grown overnight in 5 ml YPD medium, reinoculated into fresh medium at an OD_{600nm} of 0.2, and grown for 3–4 h to mid–exponential phase. Cells were collected by brief centrifugation in a microfuge, washed with double-distilled H_2O once, and spread on a 2% agarose pad in synthetic complete dextrose medium at room temperature. The samples were visualized using a deconvolution microscope (Deltavision Spectris DV4; Applied Precision) with 200-nm steps in the z axis and a 100× objective, NA 1.4 (Olympus). The micrographs were taken on a camera (CH350; Photometrics). The images were deconvoluted using Huygens deconvolution software (Scientific Volume Imaging) and generated using ImageJ.

Online supplemental material
Fig. S1 shows that the complex of His_6-Cdc12, Cdc3, Cdc10, and Shs1 produced by coexpression and copurification is stable and rod shaped. Fig. S2 provides a count of different particle sizes in the population of complexes in high salt conditions and in the population present in the background of rings in low salt. Fig. S3 demonstrates that the septin complex containing Shs1(S259D) forms disordered rings and gauzes. Fig. S4 shows that Sec3-GFP does not remain sequestered between split septin rings in shs1Δ cells as it does in WT cells. Video 1 shows that the bud neck filaments are disorganized in shs1Δ cells. Online supplemental material is available at http://www.jcb.org/cgi/content/full/jcb.201107123/DC1.

References

Abramoff, M.D., P.J. Magalhaes, and S.J. Ram. 2004. Image processing with ImageJ. *Biophotonics International*. 11:36–42.

Asano, S., J.E. Park, L.R. Yu, M. Zhou, K. Sakchaisri, C.J. Park, Y.H. Kang, J. Thorner, T.D. Veenstra, and K.S. Lee. 2006. Direct phosphorylation and activation of a Nim1-related kinase Gin4 by Elm1 in budding yeast. *J. Biol. Chem.* 281:27090–27098. http://dx.doi.org/10.1074/jbc.M601483200

Barral, Y., and M. Kinoshita. 2008. Structural insights shed light onto septin assemblies and function. *Curr. Opin. Cell Biol.* 20:12–18. http://dx.doi.org/10.1016/j.ceb.2007.12.001

Barral, Y., M. Parra, S. Bidlingmaier, and M. Snyder. 1999. Nim1-related kinases coordinate cell cycle progression with the organization of the peripheral cytoskeleton in yeast. *Genes Dev.* 13:176–187. http://dx.doi.org/10.1101/gad.13.2.176

Barral, Y., V. Mermall, M.S. Mooseker, and M. Snyder. 2000. Compartmentalization of the cell cortex by septins is required for maintenance of cell polarity in yeast. *Mol. Cell.* 5:841–851. http://dx.doi.org/10.1016/S1097-2765(00)80324-X

Barth, P., A. Schoeffler, and T. Alber. 2008. Targeting metastable coiled-coil domains by computational design. *J. Am. Chem. Soc.* 130:12038–12044. http://dx.doi.org/10.1021/ja802447e

Bertin, A., M.A. McMurray, P. Grob, S.S. Park, G. Garcia III, I. Patanwala, H.L. Ng, T. Alber, J. Thorner, and E. Nogales. 2008. *Saccharomyces cerevisiae* septins: supramolecular organization of heterooligomers and the mechanism of filament assembly. *Proc. Natl. Acad. Sci. USA*. 105:8274–8279. http://dx.doi.org/10.1073/pnas.0803330105

Byers, B., and L. Goetsch. 1976. A highly ordered ring of membrane-associated filaments in budding yeast. *J. Cell Biol.* 69:717–721. http://dx.doi.org/10.1083/jcb.69.3.717

Carroll, C.W., R. Altman, D. Schieltz, J.R. Yates, and D. Kellogg. 1998. The septins are required for the mitosis-specific activation of the Gin4 kinase. *J. Cell Biol.* 143:709–717. http://dx.doi.org/10.1083/jcb.143.3.709

De Virgilio, C., D.J. DeMarini, and J.R. Pringle. 1996. SPR28, a sixth member of the septin gene family in *Saccharomyces cerevisiae* that is expressed specifically in sporulating cells. *Microbiology*. 142:2897–2905. http://dx.doi.org/10.1099/13500872-142-10-2897

Dobbelaere, J., and Y. Barral. 2004. Spatial coordination of cytokinetic events by compartmentalization of the cell cortex. *Science*. 305:393–396. http://dx.doi.org/10.1126/science.1099892

Dobbelaere, J., M.S. Gentry, R.L. Hallberg, and Y. Barral. 2003. Phosphorylation-dependent regulation of septin dynamics during the cell cycle. *Dev. Cell*. 4:345–357. http://dx.doi.org/10.1016/S1534-5807(03)00061-3

Egelhofer, T.A., J. Villén, D. McCusker, S.P. Gygi, and D.R. Kellogg. 2008. The septins function in G1 pathways that influence the pattern of cell growth in budding yeast. *PLoS ONE*. 3:e2022. http://dx.doi.org/10.1371/journal.pone.0002022

Estey, M.P., M.S. Kim, and W.S. Trimble. 2011. Septins. *Curr. Biol.* 21:R384–R387. http://dx.doi.org/10.1016/j.cub.2011.03.067

Farkasovsky, M., P. Herter, B. Voss, and A. Wittinghofer. 2005. Nucleotide binding and filament assembly of recombinant yeast septin complexes. *Biol. Chem.* 386:643–656. http://dx.doi.org/10.1515/BC.2005.075

Fiedler, D., H. Braberg, M. Mehta, G. Chechik, G. Cagney, P. Mukherjee, A.C. Silva, M. Shales, S.R. Collins, S. van Wageningen, et al. 2009. Functional organization of the *S. cerevisiae* phosphorylation network. *Cell*. 136:952–963. http://dx.doi.org/10.1016/j.cell.2008.12.039

Fields, S. 2009. Interactive learning: lessons from two hybrids over two decades. *Proteomics*. 9:5209–5213. http://dx.doi.org/10.1002/pmic.200900236

Frank, J., M. Radermacher, P. Penczek, J. Zhu, Y. Li, M. Ladjadj, and A. Leith. 1996. SPIDER and WEB: processing and visualization of images in 3D electron microscopy and related fields. *J. Struct. Biol.* 116:190–199. http://dx.doi.org/10.1006/jsbi.1996.0030

Frazier, J.A., M.L. Wong, M.S. Longtine, J.R. Pringle, M. Mann, T.J. Mitchison, and C. Field. 1998. Polymerization of purified yeast septins: evidence that organized filament arrays may not be required for septin function. *J. Cell Biol.* 143:737–749. http://dx.doi.org/10.1083/jcb.143.3.737

Gladfelter, A.S., J.R. Pringle, and D.J. Lew. 2001. The septin cortex at the yeast mother-bud neck. *Curr. Opin. Microbiol.* 4:681–689. http://dx.doi.org/10.1016/S1369-5274(01)00269-7

Goldman, R.D., B. Grin, M.G. Mendez, and E.R. Kuczmarski. 2008. Intermediate filaments: versatile building blocks of cell structure. *Curr. Opin. Cell Biol.* 20:28–34. http://dx.doi.org/10.1016/j.ceb.2007.11.003

Golemis, E.A., I. Serebriiskii, R.L. Finley Jr., M.G. Kolonin, J. Gyuris, and R. Brent. 2011. Interaction trap/two-hybrid system to identify interacting proteins. *Curr. Protoc. Neurosci.* Chapter 4:Unit 4.4.

Haarer, B.K., and J.R. Pringle. 1987. Immunofluorescence localization of the *Saccharomyces cerevisiae* CDC12 gene product to the vicinity of the 10-nm filaments in the mother-bud neck. *Mol. Cell. Biol.* 7:3678–3687.

Hartwell, L.H. 1971. Genetic control of the cell division cycle in yeast. IV. Genes controlling bud emergence and cytokinesis. *Exp. Cell Res.* 69:265–276. http://dx.doi.org/10.1016/0014-4827(71)90223-0

Hartwell, L.H., J. Culotti, J.R. Pringle, and B.J. Reid. 1974. Genetic control of the cell division cycle in yeast. *Science*. 183:46–51. http://dx.doi.org/10.1126/science.183.4120.46

Holt, L.J., B.B. Tuch, J. Villén, A.D. Johnson, S.P. Gygi, and D.O. Morgan. 2009. Global analysis of Cdk1 substrate phosphorylation sites provides insights into evolution. *Science*. 325:1682–1686. http://dx.doi.org/10.1126/science.1172867

Hu, Q., L. Milenkovic, H. Jin, M.P. Scott, M.V. Nachury, E.T. Spiliotis, and W.J. Nelson. 2010. A septin diffusion barrier at the base of the primary cilium maintains ciliary membrane protein distribution. *Science*. 329:436–439. http://dx.doi.org/10.1126/science.1191054

Iwase, M., and A. Toh-e. 2001. Nis1 encoded by YNL078W: a new neck protein of *Saccharomyces cerevisiae*. *Genes Genet. Syst.* 76:335–343. http://dx.doi.org/10.1266/ggs.76.335

Iwase, M., J. Luo, E. Bi, and A. Toh-e. 2007. Shs1 plays separable roles in septin organization and cytokinesis in *Saccharomyces cerevisiae*. *Genetics*. 177:215–229. http://dx.doi.org/10.1534/genetics.107.073007

John, C.M., R.K. Hite, C.S. Weirich, D.J. Fitzgerald, H. Jawhari, M. Faty, D. Schläpfer, R. Kroschewski, F.K. Winkler, T. Walz, et al. 2007. The *Caenorhabditis elegans* septin complex is nonpolar. *EMBO J.* 26:3296–3307. http://dx.doi.org/10.1038/sj.emboj.7601775

Kim, S.K., A. Shindo, T.J. Park, E.C. Oh, S. Ghosh, R.S. Gray, R.A. Lewis, C.A. Johnson, T. Attie-Bittach, N. Katsanis, and J.B. Wallingford. 2010. Planar cell polarity acts through septins to control collective cell movement and ciliogenesis. *Science*. 329:1337–1340. http://dx.doi.org/10.1126/science.1191184

Kinoshita, M. 2006. Diversity of septin scaffolds. *Curr. Opin. Cell Biol.* 18:54–60. http://dx.doi.org/10.1016/j.ceb.2005.12.005

Kinoshita, M., C.M. Field, M.L. Coughlin, A.F. Straight, and T.J. Mitchison. 2002. Self- and actin-templated assembly of mammalian septins. *Dev. Cell*. 3:791–802. http://dx.doi.org/10.1016/S1534-5807(02)00366-0

Kremer, J.R., D.N. Mastronarde, and J.R. McIntosh. 1996. Computer visualization of three-dimensional image data using IMOD. *J. Struct. Biol.* 116:71–76. http://dx.doi.org/10.1006/jsbi.1996.0013

Longtine, M.S., D.J. DeMarini, M.L. Valencik, O.S. Al-Awar, H. Fares, C. De Virgilio, and J.R. Pringle. 1996. The septins: roles in cytokinesis and other processes. *Curr. Opin. Cell Biol.* 8:106–119. http://dx.doi.org/10.1016/S0955-0674(96)80054-8

Longtine, M.S., H. Fares, and J.R. Pringle. 1998. Role of the yeast Gin4p protein kinase in septin assembly and the relationship between septin assembly and septin function. *J. Cell Biol.* 143:719–736. http://dx.doi.org/10.1083/jcb.143.3.719

Ludtke, S.J., P.R. Baldwin, and W. Chiu. 1999. EMAN: semiautomated software for high-resolution single-particle reconstructions. *J. Struct. Biol.* 128:82–97. http://dx.doi.org/10.1006/jsbi.1999.4174

Mastronarde, D.N. 2008. Correction for non-perpendicularity of beam and tilt axis in tomographic reconstructions with the IMOD package. *J. Microsc.* 230:212–217. http://dx.doi.org/10.1111/j.1365-2818.2008.01977.x

McMurray, M.A., and J. Thorner. 2008. Septin stability and recycling during dynamic structural transitions in cell division and development. *Curr. Biol.* 18:1203–1208. http://dx.doi.org/10.1016/j.cub.2008.07.020

McMurray, M.A., and J. Thorner. 2009. Reuse, replace, recycle. Specificity in subunit inheritance and assembly of higher-order septin structures during mitotic and meiotic division in budding yeast. *Cell Cycle*. 8:195–203. http://dx.doi.org/10.4161/cc.8.2.7381

McMurray, M.A., A. Bertin, G. Garcia III, L. Lam, E. Nogales, and J. Thorner. 2011. Septin filament formation is essential in budding yeast. *Dev. Cell*. 20:540–549. http://dx.doi.org/10.1016/j.devcel.2011.02.004

Mino, A., K. Tanaka, T. Kamei, M. Umikawa, T. Fujiwara, and Y. Takai. 1998. Shs1p: a novel member of septin that interacts with spa2p, involved in polarized growth in *Saccharomyces cerevisiae*. *Biochem. Biophys. Res. Commun.* 251:732–736. http://dx.doi.org/10.1006/bbrc.1998.9541

Mortensen, E.M., H. McDonald, J. Yates III, and D.R. Kellogg. 2002. Cell cycle-dependent assembly of a Gin4-septin complex. *Mol. Biol. Cell*. 13:2091–2105. http://dx.doi.org/10.1091/mbc.01-10-0500

Murray, S. 2008. High pressure freezing and freeze substitution of *Schizosaccharomyces pombe* and *Saccharomyces cerevisiae* for TEM. *Methods Cell Biol.* 88:3–17. http://dx.doi.org/10.1016/S0091-679X(08)00401-9

Nagata, K.I., and M. Inagaki. 2005. Cytoskeletal modification of Rho guanine nucleotide exchange factor activity: identification of a Rho guanine nucleotide exchange factor as a binding partner for Sept9b, a mammalian septin. *Oncogene*. 24:65–76. http://dx.doi.org/10.1038/sj.onc.1208101

Nishihama, R., M. Onishi, and J.R. Pringle. 2011. New insights into the phylogenetic distribution and evolutionary origins of the septins. *Biol. Chem.* 392:681–687. http://dx.doi.org/10.1515/BC.2011.086

Nogales, E. 2000. Structural insights into microtubule function. *Annu. Rev. Biochem.* 69:277–302. http://dx.doi.org/10.1146/annurev.biochem.69.1.277

Osman, M.A., J.B. Konopka, and R.A. Cerione. 2002. Iqg1p links spatial and secretion landmarks to polarity and cytokinesis. *J. Cell Biol.* 159:601–611. http://dx.doi.org/10.1083/jcb.200205084

Ozsarac, N., M. Bhattacharyya, I.W. Dawes, and M.J. Clancy. 1995. The SPR3 gene encodes a sporulation-specific homologue of the yeast CDC3/10/11/12 family of bud neck microfilaments and is regulated by ABFI. *Gene*. 164:157–162. http://dx.doi.org/10.1016/0378-1119(95)00438-C

Pan, F.F., R.L. Malmberg, and M. Momany. 2007. Analysis of septins across kingdoms reveals orthology and new motifs. *BMC Evol. Biol.* 7:103. http://dx.doi.org/10.1186/1471-2148-7-103

Peterson, E.A., and E.M. Petty. 2010. Conquering the complex world of human septins: implications for health and disease. *Clin. Genet.* 77:511–524. http://dx.doi.org/10.1111/j.1399-0004.2010.01392.x

Pringle, J.R. 2008. Origins and development of the septin field. *In* The Septins. P.A. Hall, S.E.H. Russell, and J.R. Pringle, editors. John Wiley & Sons, Ltd, Chichester, UK. 7–34.

Rodal, A.A., L. Kozubowski, B.L. Goode, D.G. Drubin, and J.H. Hartwig. 2005. Actin and septin ultrastructures at the budding yeast cell cortex. *Mol. Biol. Cell*. 16:372–384. http://dx.doi.org/10.1091/mbc.E04-08-0734

Sanders, S.L., and C.M. Field. 1994. Cell division. Septins in common? *Curr. Biol.* 4:907–910. http://dx.doi.org/10.1016/S0960-9822(00)00201-3

Schmidt, M., A. Varma, T. Drgon, B. Bowers, and E. Cabib. 2003. Septins, under Cla4p regulation, and the chitin ring are required for neck integrity in budding yeast. *Mol. Biol. Cell*. 14:2128–2141. http://dx.doi.org/10.1091/mbc.E02-08-0547

Sellin, M.E., L. Sandblad, S. Stenmark, and M. Gullberg. 2011. Deciphering the rules governing assembly order of mammalian septin complexes. *Mol. Biol. Cell*. 22:3152–3164. http://dx.doi.org/10.1091/mbc.E11-03-0253

Shulewitz, M.J., C.J. Inouye, and J. Thorner. 1999. Hsl7 localizes to a septin ring and serves as an adapter in a regulatory pathway that relieves tyrosine phosphorylation of Cdc28 protein kinase in *Saccharomyces cerevisiae*. *Mol. Cell. Biol.* 19:7123–7137.

Sirajuddin, M., M. Farkasovsky, F. Hauer, D. Kühlmann, I.G. Macara, M. Weyand, H. Stark, and A. Wittinghofer. 2007. Structural insight into filament formation by mammalian septins. *Nature*. 449:311–315. http://dx.doi.org/10.1038/nature06052

Sirajuddin, M., M. Farkasovsky, E. Zent, and A. Wittinghofer. 2009. GTP-induced conformational changes in septins and implications for function. *Proc. Natl. Acad. Sci. USA*. 106:16592–16597. http://dx.doi.org/10.1073/pnas.0902858106

Slater, M.L., B. Bowers, and E. Cabib. 1985. Formation of septum-like structures at locations remote from the budding sites in cytokinesis-defective mutants of *Saccharomyces cerevisiae*. *J. Bacteriol.* 162:763–767.

Sung, H., K. Chul Han, J. Chul Kim, K. Wan Oh, H. Su Yoo, J. Tae Hong, Y. Bok Chung, C.K. Lee, K.S. Lee, and S. Song. 2005. A set of epitope-tagging integration vectors for functional analysis in *Saccharomyces cerevisiae*. *FEM. Yeast Res.* 5:943–950. http://dx.doi.org/10.1016/j.femsyr.2005.03.008

Takizawa, P.A., J.L. DeRisi, J.E. Wilhelm, and R.D. Vale. 2000. Plasma membrane compartmentalization in yeast by messenger RNA transport and a septin diffusion barrier. *Science*. 290:341–344. http://dx.doi.org/10.1126/science.290.5490.341

Tanaka-Takiguchi, Y., M. Kinoshita, and K. Takiguchi. 2009. Septin-mediated uniform bracing of phospholipid membranes. *Curr. Biol.* 19:140–145. http://dx.doi.org/10.1016/j.cub.2008.12.030

Tang, C.S., and S.I. Reed. 2002. Phosphorylation of the septin cdc3 in g1 by the cdc28 kinase is essential for efficient septin ring disassembly. *Cell Cycle*. 1:38–45. http://dx.doi.org/10.4161/cc.1.1.99

Versele, M., and J. Thorner. 2005. Some assembly required: yeast septins provide the instruction manual. *Trends Cell Biol.* 15:414–424. http://dx.doi.org/10.1016/j.tcb.2005.06.007

Versele, M., B. Gullbrand, M.J. Shulewitz, V.J. Cid, S. Bahmanyar, R.E. Chen, P. Barth, T. Alber, and J. Thorner. 2004. Protein-protein interactions governing septin heteropentamer assembly and septin filament organization in *Saccharomyces cerevisiae*. *Mol. Biol. Cell*. 15:4568–4583. http://dx.doi.org/10.1091/mbc.E04-04-0330

Vrabioiu, A.M., and T.J. Mitchison. 2006. Structural insights into yeast septin organization from polarized fluorescence microscopy. *Nature*. 443:466–469. http://dx.doi.org/10.1038/nature05109

Vrabioiu, A.M., and T.J. Mitchison. 2007. Symmetry of septin hourglass and ring structures. *J. Mol. Biol.* 372:37–49. http://dx.doi.org/10.1016/j.jmb.2007.05.100

Warenda, A.J., and J.B. Konopka. 2002. Septin function in *Candida albicans* morphogenesis. *Mol. Biol. Cell*. 13:2732–2746. http://dx.doi.org/10.1091/mbc.E02-01-0013

Weirich, C.S., J.P. Erzberger, and Y. Barral. 2008. The septin family of GTPases: architecture and dynamics. *Nat. Rev. Mol. Cell Biol.* 9:478–489. http://dx.doi.org/10.1038/nrm2407

Xie, Y., J.P. Vessey, A. Konecna, R. Dahm, P. Macchi, and M.A. Kiebler. 2007. The GTP-binding protein Septin 7 is critical for dendrite branching and dendritic-spine morphology. *Curr. Biol.* 17:1746–1751. http://dx.doi.org/10.1016/j.cub.2007.08.042